

# Reaction mechanisms in transport theories: a test of the nuclear effective interaction

M Colonna<sup>1</sup>, V Baran<sup>2</sup>, M Di Toro<sup>1,3</sup>, B Frecus<sup>2</sup>, YX Zhang<sup>4</sup>

<sup>1</sup>*Laboratori Nazionali del Sud, INFN, via Santa Sofia 62, I-95123, Catania, Italy*

<sup>2</sup>*Physics Faculty, University of Bucharest, Romania*

<sup>3</sup>*Physics-Astronomy Dept., University of Catania, Italy and*

<sup>4</sup>*China Institute of Atomic Energy, P.O. Box 275 (10), Beijing 102413, P.R. China*

We review recent results concerning collective excitations in neutron-rich systems and reactions between charge asymmetric systems at Fermi energies.

Solving numerically self-consistent transport equations for neutrons and protons with specific initial conditions, we explore the structure of the different dipole vibrations in the  $^{132}\text{Sn}$  system and investigate their dependence on the symmetry energy. We evidence the existence of a distinctive collective mode, that can be associated with the Pygmy Dipole Resonance, with an energy well below the standard Giant Dipole Resonance and isoscalar-like character, i.e. very weakly dependent on the isovector part of the nuclear effective interaction. At variance, the corresponding strength is rather sensitive to the behavior of the symmetry energy below saturation, which rules the number of excess neutrons in the nuclear surface.

In reactions between charge asymmetric systems at Fermi energies, we investigate the interplay between dissipation mechanisms and isospin effects. Observables sensitive to the isospin dependent part of nuclear interaction are discussed, providing information on the symmetry energy density dependence below saturation.

## I. INTRODUCTION

The Equation of State (EOS) of nuclear matter is of crucial importance for the understanding of a large variety of phenomena in nuclear physics and astrophysics. Transient states of nuclear matter far from normal conditions can be created in terrestrial laboratories and many experimental and theoretical efforts have been devoted to the study of nuclear reactions, from low to intermediate energies, as a possible tool to learn about the behavior of nuclear matter and its EOS. In particular, the availability of exotic beams has opened the way to explore, in laboratory conditions, new aspects of nuclear structure and dynamics up to extreme ratios of neutron (N) to proton (Z) numbers. Over the past years, measurements of isoscalar collective vibrations, collective flows and meson production have contributed to constrain the EOS for symmetric matter for densities up to five times the saturation value [1]. However, the EOS of asymmetric matter has comparatively few experimental constraints: The isovector part of the nuclear effective interaction (Asy-EOS) and the corresponding symmetry energy are largely unknown far from normal density.

This information is essential also in the astrophysical context, for the understanding of the properties of compact objects such as neutron stars, whose crust behaves as low-density asymmetric nuclear matter [2] and whose core may touch extreme values of density and asymmetry. Moreover, the low-density behavior of the symmetry energy also affects the structure of exotic nuclei and the appearance of new features involving the neutron skin [3].

Over the past years, several observables which are sensitive to the Asy-EOS and testable experimentally, have been suggested [4–7].

In this contribution we will focus on some effects related to the low-density sector of the nuclear EOS. The first part will be devoted to the study of collective excitations in neutron-rich systems. New exotic collective modes show up when one moves away from the valley of stability [8]. In particular, we will discuss results concerning the appearance of an interesting exotic mode, the Pygmy Dipole Resonance (PDR), which was observed as an unusually large concentration of the dipole response at energies clearly below the values associated with the standard Giant Dipole Resonance (GDR). Then, in the second part, we will discuss dissipation and fragmentation mechanisms at Fermi energies, concentrating on isospin effects and on the sensitivity of detectable observables to the Asy-EOS.

## II. TRANSPORT THEORIES AND SYMMETRY ENERGY

Nuclear collective motion and nuclear reactions are modeled by solving transport equations based on mean field theories, with correlations included via hard nucleon-nucleon elastic collisions and via stochastic forces, selfconsistently evaluated from the mean phase-space trajectory, see [5, 9]. Stochasticity is essential in order to get distributions as well as to allow for the growth of dynamical instabilities.

In the beam energy range up to a few hundred  $MeV/u$ , the appropriate tool is the so-called Boltzmann-Langevin equation (BLE) [9]:

$$\frac{df}{dt} = \frac{\partial f}{\partial t} + \{f, H\} = I_{coll}[f] + \delta I[f], \quad (1)$$

where  $f(\mathbf{r}, \mathbf{p}, t)$  is the one-body distribution function, the semi-classical analog of the Wigner transform of the one-body density,  $H(\mathbf{r}, \mathbf{p}, t)$  the mean field Hamiltonian,  $I_{coll}$  the two-body collision term incorporating the Fermi statistics of the particles, and  $\delta I[f]$  the fluctuating part of the collision integral. Here we follow the approximate treatment to the BLE introduced in [10], the so-called Stochastic Mean Field (SMF) model, where fluctuations are injected just in coordinate space by agitating the density profile.

The symmetry energy,  $E_{sym}$ , appears in the energy density  $\epsilon(\rho, \rho_i) \equiv \epsilon(\rho) + \rho E_{sym}/A (\rho_i/\rho)^2 + O(\rho_i/\rho)^4 + \dots$ , expressed in terms of total ( $\rho = \rho_p + \rho_n$ ) and isospin ( $\rho_i = \rho_p - \rho_n$ ) densities.  $E_{sym}$  gets a kinetic contribution directly from basic Pauli correlations and a potential part,  $C(\rho)$ , from the highly controversial isospin dependence of the effective interactions:

$$\frac{E_{sym}}{A} = \frac{E_{sym}}{A}(kin) + \frac{E_{sym}}{A}(pot) \equiv \frac{\epsilon_F}{3} + \frac{C(\rho)}{2\rho_0}\rho. \quad (2)$$

The sensitivity of the simulation results can be tested against different choices of the density dependence of the coefficient  $C(\rho)$ .

### III. COLLECTIVE EXCITATIONS IN NEUTRON-RICH SYSTEMS

One of the important tasks in many-body physics is to understand the emergence of the collective features as well as their structure in terms of the individual motion of the constituents. The experimental characterization and theoretical description of new exotic collective excitations is a challenge for modern nuclear physics. Recent experiments provided several evidences about their existence but the available information is still incomplete and their nature is a matter of debate. In particular, many efforts have been devoted to the study of the PDR, identified as an unusually large concentration of the dipole response at energies below the values corresponding to the GDR. The latter is one of the most prominent and robust collective motions, present in all nuclei, whose centroid position varies, for medium-heavy nuclei, as  $80A^{-1/3}MeV$ . From a comparison of the available data for stable and unstable  $Sn$  isotopes a correlation between the fraction of pygmy strength and isospin asymmetry was noted [11]. In general the exhausted sum-rule increases with the proton-to-neutron asymmetry. This behavior was related to the symmetry energy properties below saturation and therefore connected to the size of the neutron skin [3, 12, 13].

In spite of the theoretical progress in the interpretation of this mode and new experimental information [14–17], a number of critical questions concerning the nature of the PDR still remains. Our goal is to address the important issue related to the collective nature of the PDR in connection with the role of the symmetry energy.

An accurate picture of the GDR in nuclei corresponds to an admixture of Goldhaber-Teller (G-T) and Stenweidel-Jensen (S-J) vibrations. The latter, in symmetric nuclear matter, is a volume type oscillation of the isovector density  $\rho_i = \rho_n - \rho_p$  keeping the total density  $\rho = \rho_n + \rho_p$  constant [18]. A microscopic, self-consistent study of the collective features and of the role of the nuclear effective interaction upon the PDR can be performed within the Landau theory of Fermi liquids. This is based on two coupled Landau-Vlasov kinetic equations (see Eq.(1), neglecting the stochastic term) for neutron and proton one-body distribution functions  $f_q(\vec{r}, \vec{p}, t)$  with  $q = n, p$ , and was applied quite successfully in describing various features of the GDR, including pre-equilibrium dipole excitation in fusion reactions [19]. However, it should be noticed that within such a semi-classical description shell effects are absent, certainly important in shaping the fine structure of the dipole response [20]. By solving numerically the Vlasov equation in the absence of Coulomb interaction, Urban [21] evidenced from the study of the total dipole moment  $D$  a collective response around  $8.6 MeV$  which was identified as a pygmy mode. It was pointed out, from the properties of transition densities and velocities, that the PDR can be related to one of the low-lying modes associated with isoscalar toroidal excitations, providing indications about its isoscalar character. Here, considering in the transport simulations also the Coulomb interaction, we shall investigate in a complementary way the collective nature of PDR by studying the dynamics of the pygmy degree of freedom,  $D_y$ , that is usually associated with the neutron excess in the nuclear surface [22]. Moreover, we shall explore the isoscalar character of the mode by a comparative analysis employing three different density parametrizations of the symmetry energy.

asy-EoS	$E_{sym}/A$	$L(\text{MeV})$	$R_n(\text{fm})$	$R_p(\text{fm})$	$\Delta R_{np}(\text{fm})$
asysoft	29.9	14.4	4.90	4.65	0.25
asystiff	28.3	72.6	4.95	4.65	0.30
asysupstiff	28.3	96.6	4.96	4.65	0.31

TABLE I: The symmetry energy at saturation (in  $\text{MeV}$ ), the slope parameters, neutron rms radius, protons rms radius, neutron skin thickness for the three Asy-EOS.

### A. Ingredients of the simulations

We neglect the two-body collision effects and hence the main ingredient of the dynamics is the nuclear mean-field, for which we consider a Skyrme-like ( $SKM^*$ ) parametrization  $U_q = A \frac{\rho}{\rho_0} + B \left(\frac{\rho}{\rho_0}\right)^{\alpha+1} + C(\rho) \frac{\rho_n - \rho_p}{\rho_0} \tau_q + \frac{1}{2} \frac{\partial C}{\partial \rho} \frac{(\rho_n - \rho_p)^2}{\rho_0}$ , where  $\tau_q = +1(-1)$  for  $q = n(p)$  and  $\rho_0$  denotes the saturation density. The saturation properties of symmetric nuclear matter are reproduced with the values of the coefficients  $A = -356.8 \text{ MeV}$ ,  $B = 303.9 \text{ MeV}$ ,  $\alpha = 1/6$ , leading to a compressibility modulus  $K = 201 \text{ MeV}$ . For the isovector sector we employ three different parameterizations of  $C(\rho)$  with the density: the asysoft, the asystiff and asysuperstiff respectively, see [5] for a detailed description. The value of the symmetry energy,  $E_{sym}/A$ , at saturation, as well as the slope parameter,  $L = 3\rho_0 \frac{dE_{sym}/A}{d\rho}|_{\rho=\rho_0}$ , are reported in Table I for each of these Asy-EOS. Just below the saturation density the asysoft mean field has a weak variation with density while the asysuperstiff shows a rapid decrease. Then, due to surface contributions to the collective oscillations, we expect to see some differences in the energy position of the dipole response of the system.

The numerical procedure to integrate the transport equations is based on the test-particle (t.p.) method. For a good spanning of phase-space we work with 1200 t.p. per nucleon. We consider the neutron rich nucleus  $^{132}\text{Sn}$  and we determine its ground state configuration as the equilibrium (static) solution of Eq.(1). Then proton and neutron densities  $\rho_q(\vec{r}, t) = \int \frac{2d^3\mathbf{p}}{(2\pi\hbar)^3} f_q(\vec{r}, \vec{p}, t)$  can be evaluated. As an additional check of our initialization procedure, the neutron and proton mean square radii  $\langle r_q^2 \rangle = \frac{1}{N_q} \int r^2 \rho_q(\vec{r}, t) d^3\mathbf{r}$ , as well as the skin thickness  $\Delta R_{np} = \sqrt{\langle r_n^2 \rangle} - \sqrt{\langle r_p^2 \rangle}$ , were also calculated in the ground state and shown in Table I. The values obtained with our semi-classical approach are in a reasonable agreement with those reported by employing other models for similar interactions [23]. The neutron skin thickness is increasing with the slope parameter, as expected from a faster reduction of the symmetry term on the surface [5, 12]. This feature has been discussed in detail in [3].

To inquire on the collective properties of the pygmy dipole we excite the nuclear system at the initial time  $t = t_0 = 30 \text{ fm}/c$  by boosting along the  $z$  direction all excess neutrons ( $N_e = 32$ ) and in opposite direction all core nucleons, while keeping the 'c.m.' of the nucleus at rest (Pygmy-like initial conditions). The excess neutrons were identified as the most distant  $N_e = 32$  neutrons from the nucleus CM. Then the system is left to evolve and the evolution of the collective coordinates  $Y$ ,  $X_c$  and  $X$ , associated with the different isovector dipole modes (pygmy, core and total dipole) is followed for  $600 \text{ fm}/c$  by solving numerically the equations (1). During the time evolution the number of t. p. escaping from the system corresponds, on average, to less than half a neutron, while the total energy conservation is satisfied within 1.5%.

### B. Results for dipole oscillations

As shown in figure 1, apart from the quite undamped oscillations of the  $Y$  coordinate, we also remark that the core does not remain inert. We plot the time evolution of the dipole  $D_y$ , of the total dipole  $D$  and core dipole  $D_c$  moments, for two Asy-EoS. As observed, while  $D_y$  approaches its maximum value, an oscillatory motion of the dipole  $D_c$  initiates and this response is symmetry energy dependent: the larger is the slope parameter  $L$ , the more delayed is the isovector core reaction. This can be explained in terms of low-density (surface) contributions to the vibration and therefore of the density behavior of the symmetry energy below normal density: a larger  $L$  corresponds to a larger neutron presence in the surface and so to a smaller coupling to the core protons. We see that the total dipole  $D(t)$  is strongly affected by the presence of isovector core oscillations, mostly related to the isovector part of the effective interaction. Indeed,  $D(t)$  gets a higher oscillation frequency with respect to  $D_y$ , sensitive to the Asy-EoS. The fastest vibrations are observed in the asysoft case, which gives the largest value of the symmetry energy below saturation.

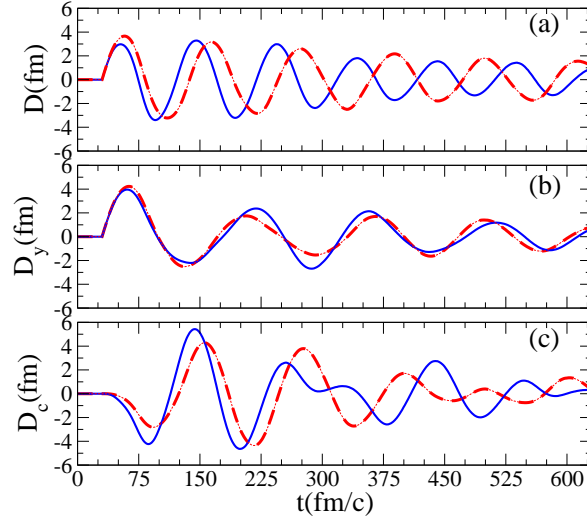


FIG. 1: (Color online) The time evolution of the total dipole  $D$  (a), of the dipole  $D_y$  (b) and of core dipole  $D_c$  (c), for asysoft (the blue (solid) lines) and asysuperstiff (the red (dashed) lines) EOS. Pygmy-like initial excitation.

In correspondence the frequency of the pygmy mode seems to be not much affected by the trend of the symmetry energy below saturation, see also next figure 2, clearly showing the different nature, isoscalar-like, of this oscillation.

For each case we calculate the power spectrum of  $D_y$ :  $|D_y(\omega)|^2 = \left| \int_{t_0}^{t_{max}} D_y(t) e^{-i\omega t} dt \right|^2$  and similarly for  $D$ . The results are shown in figure 2. The position of the centroid corresponding to the GDR shifts toward larger values when we move from asysuperstiff (largest slope parameter  $L$ ) to asysoft EOS. This evidences the importance of the volume, S-J component of the GDR in  $^{132}\text{Sn}$ . The energy centroid associated with the PDR is situated below the GDR peak, at around  $8.5\text{MeV}$ , quite insensitive to the Asy-EOS, pointing to an isoscalar-like nature of this mode. Hence the structure of the dipole response can be explained in terms of the development of isoscalar-like (PDR) and isovector-like (GDR) modes, as observed in asymmetric systems [24]. Both modes are excited in the considered pygmy-like initial

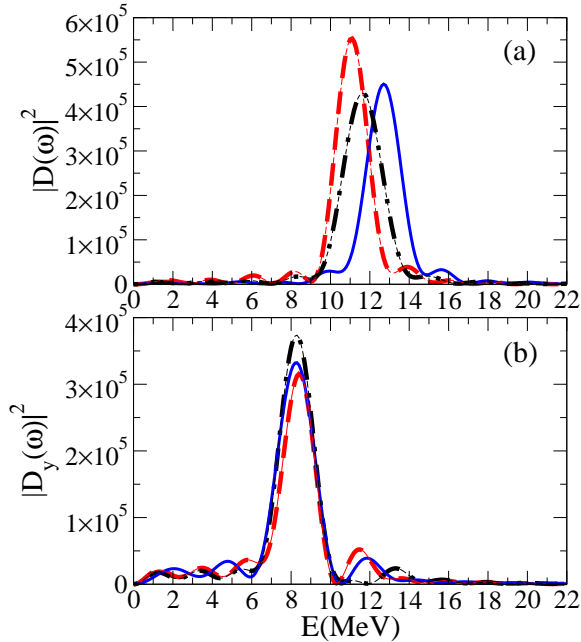


FIG. 2: (Color online) The power spectrum of total dipole (a) and of the dipole  $D_y$  (b) (in  $\text{fm}^4/c^2$ ), for asysoft (the blue (solid) lines), asystiff (the black (dot-dashed) lines) and asysuperstiff (the red (dashed) lines) EOS. Pygmy-like initial conditions.

conditions. Looking at the total dipole mode direction, that is close to the isovector-like normal mode, one observes a quite large contribution in the GDR region. On the other hand, although the pygmy mode has a more complicated

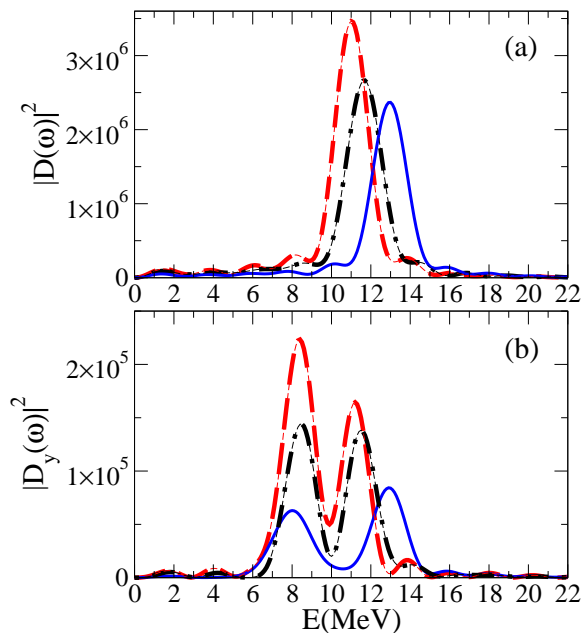


FIG. 3: (Color online) The same as in figure 2 but for a GDR-like initial excitation.

structure [21], the  $Y$  direction appears closely related to it. Indeed a larger response amplitude is detected in the pygmy region, see figure 2 (bottom).

To check the influence of the initial conditions on the dipole response, let us consider the case of a GDR-like excitation, corresponding to a boost of all neutrons against all protons, keeping the CM at rest. Now the initial excitation favors the isovector-like mode and even in the  $Y$  direction we observe a sizable contribution in the GDR region, see the Fourier spectrum of  $D_y$  in figure 3. From this result it clearly emerges that a part of the  $N_e$  excess neutrons is involved in a GDR type motion and the relative weight depends on the symmetry energy: more neutrons are involved in the pygmy mode in the asysuperstiff EOS case, in connection to the larger neutron skin size. We have also checked that, if the coordinate  $Y$  is constructed by taking the  $N_y$  most distant neutrons (with  $N_y < N_e$ ), the relative weight increases in the PDR region. In any case, since part of the excess nucleons contributes to the GDR mode, a low EWSR value is expected in the PDR region. Indeed, in the Fourier power spectrum of  $D$  in figure 3, a weak response is seen at the pygmy frequency. In the case of the GDR-like initial excitation, i.e. boosting all neutrons against all protons, we can relate the strength function to  $Im(D(\omega))$  [25] and then the corresponding cross section can be calculated. Our estimate of the integrated cross section over the PDR region represents 2.7% for asysoft, 4.4% for asystiff and 4.5% for asysuperstiff, out of the total cross section. Hence the EWSR exhausted by the PDR is proportional to the skin thickness, in agreement with the results of [26].

#### IV. ISOSPIN EQUILIBRATION AND FRAGMENTATION MECHANISMS AT FERMI ENERGIES

In this energy range, reactions between charge asymmetric systems are characterized by a direct isospin transport in binary events. This process also involves the low density neck region and is sensitive to the low density behavior of  $E_{sym}$ , see Refs.[27, 28] and references therein. Moreover, it is now quite well established that the largest part of the reaction cross section for dissipative collisions at Fermi energies goes through the *Neck Fragmentation* channel, with intermediate mass fragments (IMF) directly produced in the interacting zone in semiperipheral collisions on short time scales [30]. It is possible to predict interesting isospin transport effects also for this fragmentation mechanism since clusters are formed still in a dilute asymmetric matter but always in contact with the regions of the projectile-like and target-like remnants almost at normal densities.

Results on these mechanisms, obtained with the SMF model, are discussed below.

##### A. The isospin transport ratio

In peripheral and semi-peripheral reactions, it is interesting to look at the asymmetries of the various parts of the interacting system in the exit channel: emitted particles, projectile-like (PLF) and target-like fragments (TLF), and in the case of ternary (or higher multiplicity) events, IMF's. In particular, one can study the so-called isospin

transport ratio, which is defined as

$$R_{P,T}^x = \frac{2(x^M - x^{eq})}{(x^H - x^L)}, \quad (3)$$

with  $x^{eq} = \frac{1}{2}(x^H + x^L)$ . Here,  $x$  is an isospin sensitive quantity that has to be investigated with respect to equilibration. We consider primarily the asymmetry  $\beta = I = (N - Z)/A$ , but also other quantities, such as isoscaling coefficients, ratios of production of light fragments, etc., can be of interest [6]. The indices  $H$  and  $L$  refer to the symmetric reaction between the heavy ( $n$ -rich) and the light ( $n$ -poor) systems, while  $M$  refers to the mixed reaction.  $P, T$  denote the rapidity region, in which this quantity is measured, in particular the PLF and TLF rapidity regions. Clearly, this ratio is  $\pm 1$  in the projectile and target regions, respectively, for complete transparency, and oppositely for complete rebound, while it is zero for complete equilibration.

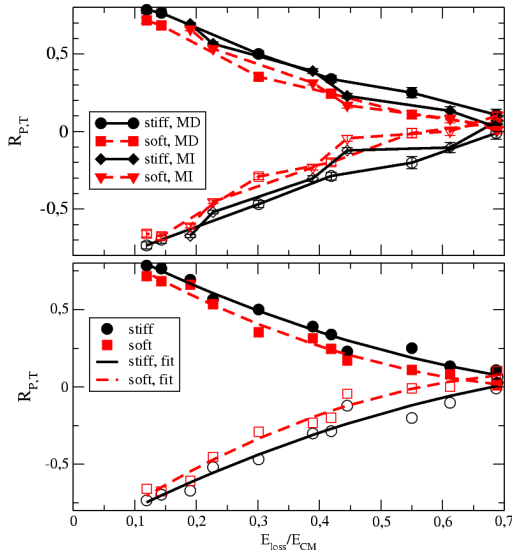


FIG. 4: Isospin transport ratios as a function of relative energy loss. Upper panel: separately for stiff (solid) and soft (dashed) Asy-EOS, and for two parameterizations of the isoscalar part of the interaction: MD (circles and squares) and MI (diamonds and triangles), in the projectile region (full symbols) and the target region (open symbols). Lower panel: quadratic fit to all points for the stiff (solid), resp. soft (dashed) Asy-EOS.

In a simple model one can show that the isospin transport ratio mainly depends on two quantities: the strength of the symmetry energy and the interaction time between the two reaction partners. Let us take, for instance, the asymmetry  $\beta$  of the PLF (or TLF) as the quantity  $x$ . At a first order approximation, in the mixed reaction this quantity relaxes towards its complete equilibration value,  $\beta_{eq} = (\beta_H + \beta_L)/2$ , as

$$\beta_{P,T}^M = \beta^{eq} + (\beta^{H,L} - \beta^{eq}) e^{-t/\tau}, \quad (4)$$

where  $t$  is the time elapsed while the reaction partners stay in contact (interaction time) and the damping  $\tau$  is mainly connected to the strength of the symmetry energy [28]. Inserting this expression into Eq.(3), one obtains  $R_{P,T}^\beta = \pm e^{-t/\tau}$  for the PLF and TLF regions, respectively. Hence the isospin transport ratio can be considered as a good observable to trace back the strength of the symmetry energy from the reaction dynamics provided a suitable selection of the interaction time is performed. The centrality dependence of the isospin ratio, for Sn + Sn collisions at 35 and 50 MeV/u, has been investigated in experiments as well as in theory [27–29], and information about the stiffness of the symmetry energy has been extracted from the analysis presented in [29], based on the ImQMD model.

Here we investigate more in detail the relation between charge equilibration, interaction times and thermal equilibrium. Longer interaction times should be correlated to a larger dissipation. It is then natural to look at the correlation between the isospin transport ratio and the total kinetic energy loss. In this way one can also better disentangle dynamical effects of the isoscalar and isovector part of the EOS, see [28].

It is seen in figure 4 (top) that the curves for the asysoft EOS (dashed) are generally lower in the projectile region (and oppositely for the target region), i.e. show more equilibration, than those for the asystiff EOS, due to the higher value of the symmetry energy at low density. To emphasize this trend, all the values for the stiff (circles) and the soft (squares) Asy-EOS, corresponding to different impact parameters, beam energies and also to two possible parameterizations of the isoscalar part of the nuclear interaction (with and without momentum dependence, MD and MI), are collected together in the bottom part of the figure. One can see that all the points essentially follow a given line, depending only on the symmetry energy parameterization adopted. It is seen, that there is a systematic effect

of the symmetry energy of the order of about 20 percent, which should be measurable. Moreover, we notice that the quantity  $R$  is a rapidly decreasing function of the degree of dissipation,  $E_{loss}$ , reached in the collision. This can be explained in terms of dissipation mechanisms mainly due to mean-field effects, as predicted by the SMF model. Indeed, according to a mean-field picture, a significant degree of thermal equilibrium (i.e. a considerable  $E_{loss}$ ) would imply a rather long contact time between the two reaction partners, thus certainly leading to isospin equilibration, that needs a shorter time scale to be reached. The correlation suggested in figure 4 should represent a general feature of isospin diffusion, as expected on the basis of dominant mean-field mechanisms, and it would be of great interest to verify it experimentally.

### B. Isospin dynamics in neck fragmentation at Fermi energies

In presence of density gradients, as the ones occurring when a low-density neck region is formed between the two reaction partners in semi-peripheral collisions, the isospin transport is mainly ruled by the density derivative of the symmetry energy and so we expect a larger neutron flow to the neck clusters for a stiffer symmetry energy around saturation [5]. This mechanism leads to the neutron enrichment of the neck region (isospin migration). This is shown in figure 5 (left), where the asymmetry of the neck and PLF-TLF regions, obtained in neutron-rich reactions at 50 MeV/u, are plotted for two Asy-EOS choices.

From the experimental point of view, a new analysis has been recently published on Sn+Ni data at 35 MeV/u by the Chimera Collab.[32]. A strong correlation between neutron enrichment and fragment alignment (when the short emission time selection is enforced) is seen, that points to a stiff behavior of the symmetry energy ( $L \approx 70$  MeV), for which a large neutron enrichment of neck fragments is seen (left).

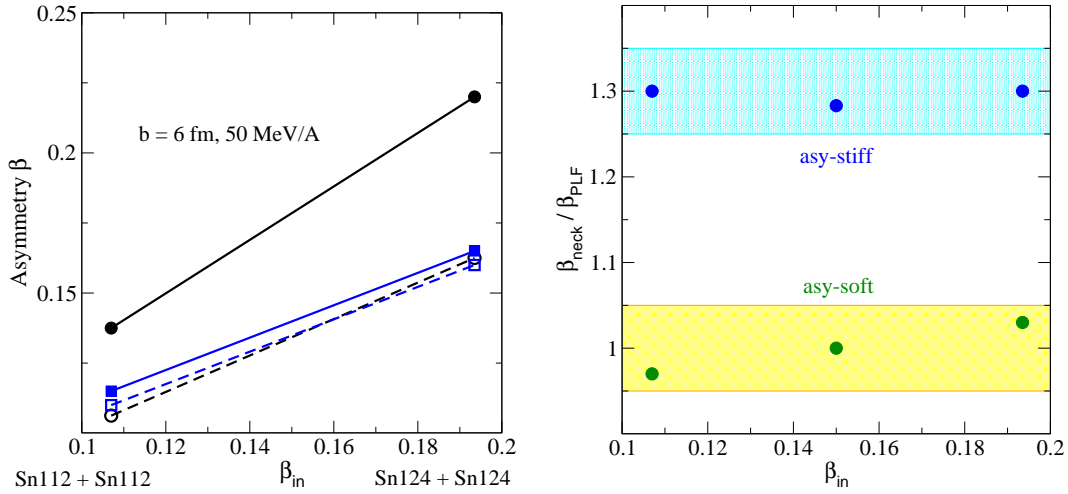


FIG. 5: Left panel: asymmetry of IMF's (circles) and PLF-TLF (squares), as a function of the system initial asymmetry, for two Asy-EOS choices: asystiff (full lines) and asysoft (dashed lines). Right panel: Ratio between the neck IMF and the PLF asymmetries, as a function of the system initial asymmetry. The bands indicate the uncertainty in the calculations.

In order to build observables less affected by secondary decay effects, in fig. 5 (right) we consider the ratio of the asymmetries of the IMF's to those of the residues ( $\beta_{res}$ ) for stiff and soft Asy-EOS. This quantity can be estimated on the basis of simple energy balance considerations. By imposing to get a maximum (negative) variation of  $E_{sym}$  when transferring the neutron richness from PLF and TLF towards the neck region, one obtains:

$$\frac{\beta_{IMF}}{\beta_{res}} = \frac{E_{sym}(\rho_R)}{E_{sym}(\rho_I)} \quad (5)$$

From this simple argument the ratio between the IMF and residue asymmetries should depend only on symmetry energy properties and, in particular, on the difference of the symmetry energy corresponding to the residue and neck densities ( $\rho_R$  and  $\rho_I$ ), as appropriate for isospin migration. It should also be larger than one, more so for the asystiff than for the asysoft EOS. It is seen indeed in figure 5 (right part), that this ratio is nicely dependent on the Asy-EOS

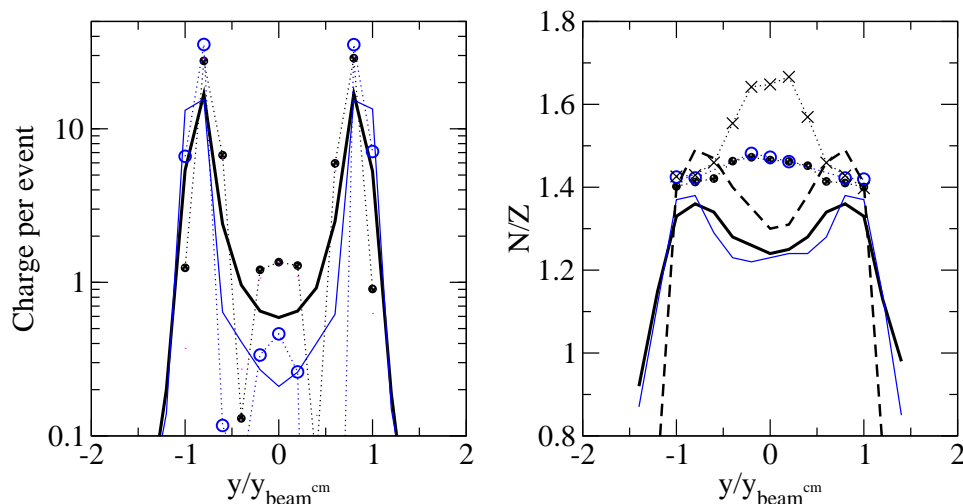


FIG. 6: Left panel: Average total charge per event, associated with IMF's, as a function of the reduced rapidity, obtained in the reaction  $^{124}\text{Sn} + ^{124}\text{Sn}$  at 50 MeV/u. Results are shown for ImQMD calculations at  $b = 6$  fm (thick line) and  $b = 8$  fm (thin line) and for SMF calculations at  $b = 6$  fm (full circles) and  $b = 8$  fm (open circles). A soft interaction is considered for the symmetry energy. Right panel:  $N/Z$  of IMF's as a function of the reduced rapidity. Lines and symbols are like in the left panel. Results corresponding to a stiff asy-EOS are also shown for ImQMD (dashed line) and SMF (crosses), for  $b=6$  fm.

only (being larger in the asystiff case) and not on the system considered. If final asymmetries were affected in the same way by secondary evaporation in the case of neck and PLF fragments, then one could directly compare the results of figure 5 (right) to data. However, due to the different size and temperature of the neck region with respect to PLF or TLF sources, de-excitation effects should be carefully checked with the help of suitable decay codes.

### C. Comparison with the predictions of different transport codes

A detailed investigation of isospin equilibration has been recently undertaken within transport codes based on the molecular dynamics (QMD) approach [29]. In comparison to the transport models considered before, mainly describing one-body effects (such as the SMF model, see Eq.(1)), such approaches, where nucleons are represented as individual wave packets of fixed compact shape (usually taken as gaussians), may lead to approximate descriptions of mean-field effects. On the other hand, fluctuations and correlations should be well reproduced, especially in the exit channel of multifragmentation events. As shown in Ref.[29], where charge equilibration is investigated for  $Sn + Sn$  reactions at 35 and 50 MeV/u, the ImQMD code predicts a quite different behavior with respect to SMF: the isospin transport ratio exhibits a rather flat behavior as a function of the impact parameter. This seems to indicate that, even in the case of central collisions, the contact time between the two reaction partners remains rather short, the dissipation mechanisms being mostly due to many-body correlations rather than to mean-field effects. Thus the more explosive dynamics would lead to the lower degree of isospin equilibration observed.

To examine more in detail the origin of the observed discrepancies, results concerning IMF ( $Z > 2$ ) properties, obtained with the SMF and ImQMD codes, are compared in figure 6. In the left panel, the average total charge per event, associated with IMF's, is plotted as a function of the reduced rapidity, for the reaction  $^{124}\text{Sn} + ^{124}\text{Sn}$  at 50 MeV/u and impact parameters  $b = 6$  and 8 fm. From this comparison it is clear that in ImQMD a larger number of light IMF's, distributed over all rapidity range between PLF and TLF, are produced. On the other hand, mostly binary or ternary events are observed in SMF, with light IMF's located very close to mid-rapidity. Then the different reaction dynamics predicted by the two codes may explain the different results seen for isospin equilibration especially in semi-peripheral and central reactions ( $b \approx 4-6$  fm). The fast ImQMD fragmentation dynamics inhibits nucleon exchange and charge equilibration. On the other hand, in SMF dissipation is dominated by mean-field mechanisms, acting over longer time intervals and leading to stronger equilibration effects. Results on the neutron content of the neck region are illustrated in the right panel of figure 6, that shows the global  $N/Z$  of IMF's as a function of the reduced rapidity. As discussed above, SMF calculations clearly predict a larger  $N/Z$  for IMF's produced at mid-rapidity, with respect to PLF and TLF regions (isospin migration effect). The effect is particularly pronounced in the case of the asystiff parametrization. On the contrary, ImQMD calculations predict a minimum of the  $N/Z$  ratio at mid-rapidity.



The reasons of the these differences need to be further investigated.

## V. CONCLUSIONS

We have reviewed some aspects of the rich phenomenology associated with nuclear reactions, from which interesting hints are emerging to constrain the nuclear EOS and, in particular, the largely debated density behavior of the symmetry energy. Information on the low density region can be accessed in reactions from low to intermediate energies, where collective excitations and fragmentation mechanisms are dominant.

We have shown, within a semi-classical Landau-Vlasov approach, the existence, in neutron rich nuclei, of a collective pygmy dipole mode determined by the oscillations of some excess neutrons against the nuclear core. From the transport simulations the PDR energy centroid for  $^{132}\text{Sn}$  appears around 8.5 MeV, rather insensitive to the density dependence of the symmetry energy and well below the GDR peak. This supports the isoscalar-like character of this collective motion. A complex pattern, involving the coupling of the neutron skin with the core dipole mode, is noticed. This reduces considerably the EWSR acquired by the PDR, our numerical estimate providing values well below 10%, but proportional to the symmetry energy slope parameter  $L$ , that affects the number of excess neutrons on the nuclear surface.

Concerning nuclear reactions at Fermi energies, we have discussed some results on isospin sensitive observables. In particular, we have concentrated our analysis on the charge equilibration mechanism (and its relation to energy dissipation) and on the neutron-enrichment of the neck region in semi-peripheral reactions. From the study of the latter mechanism, for which new experimental evidences have recently appeared [32], hints are emerging towards a stiff behavior of the symmetry energy around normal density. This is compatible with recent results from structure data, see for instance the review article [33].

Finally, we have also considered results of different transport codes (see section 4.3), undertaking a comparison of ImQMD and SMF predictions for selected observables. Due to the different role of mean-field effects, vs. fluctuations and many-body correlations, in the two codes, the description of the reaction dynamics is model dependent (see also [34]). This affects also isospin sensitive observables. Thus the whole reaction path needs to be carefully checked against experimental data in order to get decisive conclusions about the density dependence of the symmetry energy.

## Acknowledgements

We warmly thank H.Wolter and M.Zielinska-Pfabe for inspiring discussions.

This work for V. Baran was supported by a grant of the Romanian National Authority for Scientific Research, CNCS - UEFISCDI, project number PN-II-ID-PCE-2011-3-0972. For B. Frecus this work was supported by the strategic grant POSDRU/88/1.5/S/56668.

- 
- [1] Danielewicz P, Lacey R and Lynch WG 2002 *Science* **298** 1592
  - [2] Lattimer JM and Prakash M 2007 *Phys.Rep* **442**
  - [3] Carbone A *et al* 2010 *Phys. Rev.* **C81** 041301
  - [4] *Isospin Physics in Heavy-ion Collisions at Intermediate Energies*, Eds. Li BA and Schröder WU, Nova Science Publishers (2001, New York)
  - [5] Baran V, Colonna M, Greco V and Di Toro M 2005 *Phys. Rep.* **410** 335
  - [6] Colonna M and Tsang MB 2006 *Eur. Phys. J A* **30** 165, and references therein
  - [7] Li BA, Chen LW and Ko CM 2008 *Phys. Rep.* **465** 113
  - [8] Paar N, Vretenar D, Khan E, Coló G 2007 *Rep. Prog. Phys* **70** 691
  - [9] Chomaz P, Colonna M and Randrup J 2004 *Phys. Rep.* **389** 263
  - [10] Colonna M *et al* 1998 *Nucl. Phys.* **A642** 449; Rizzo J, Chomaz Ph, Colonna M 2008 *Nucl. Phys.* **A806** 40 and references therein
  - [11] Klimkiewicz A *et al* 2007 *Phys. Rev.* **C76** 051603(R)
  - [12] Yoshida S, Sagawa H 2004 *Phys. Rev.* **C69** 024318; 2006 *Phys. Rev.* **C73** 044320
  - [13] Piekarewicz J 2006 *Phys. Rev.* **C73** 044325
  - [14] Savran D *et al* 2008 *Phys. Rev. Lett.* **100** 232501
  - [15] Wieland O *et al* 2010 *Phys. Rev. Lett.* **102** 092502; Wieland O, Bracco A 2011 *Prog.Part. Nucl. Phys.* **66** 304; Toft HK *et al* 2010 *Phys. Rev.* **C81** 064311

- [16] Tonchev AP *et al* 2010 *Phys. Rev. Lett.* **104** 072501
- [17] Makinaga A *et al* 2010 *Phys. Rev.* **C82** 024314
- [18] Steinwedel H, Jensen JHD 1950 *Z. Naturf.* **5A** 413
- [19] Baran V, Rizzo C, Colonna M, Di Toro M, Pierroutsakou D 2009 *Phys. Rev.* **C79** 021603(R)
- [20] Roca-Maza X, Pozzi G, Brenna M, Mizuyama K, Coló G 2012 *Phys. Rev.* **C85** 024601
- [21] Urban M 2012 *Phys. Rev.* **C85** 034322
- [22] Baran V, Frecus B, Colonna M and Di Toro M 2012 *Phys. Rev.* **C85** 051601(R)
- [23] Paar N, Nicsik T, Vretenar D, Ring P 2005 *Phys. Lett.* **B606** 288
- [24] Baran V, Colonna M, Di Toro M, Greco V 2001 *Phys. Rev. Lett.* **86** 4492; Colonna M, Chomaz P, Ayik S 2002 *Phys. Rev. Lett.* **88** 122701
- [25] Calvayrac F, Reinhard PG, Suraud E 1997 *Ann. Phys.* **225** 125
- [26] Inakura T, Nakatsukasa T, Yabana K 2011 *Phys. Rev.* **C84** 021302(R)
- [27] Tsang MB *et al* 2004 *Phys. Rev. Lett.* **92** 062701
- [28] Rizzo J *et al* 2008 *Nucl. Phys. A* **806** 79
- [29] Tsang MB *et al* 2009 *Phys. Rev. Lett.* **102** 122701; Sun ZY *et al* 2010 *Phys. Rev.* **C82** 051603
- [30] Di Toro M, Olmi A and Roy R 2006 *Eur. Phys. Jour.* **A30** 65
- [31] Tsang MB *et al* 2011 *Prog. Part. Nucl. Phys.* **66** 400
- [32] De Filippo E *et al* (Chimera Collab.) 2012 *Phys. Rev.* **C86** 014610
- [33] Tsang MB *et al* 2012 arXiv:1204.0466
- [34] Coupland D *et al* 2011 *Phys. Rev.* **C84** 054603